Solid-State Electronics 75 (2012) 93–96

Contents lists available at SciVerse ScienceDirect

Solid-State Electronics

journal homepage: www.elsevier.com/locate/sse

Investigation on the relationship between channel resistance and subgap density of states of amorphous InGaZnO thin film transistors

Suehye Park, Edward Namkyu Cho, Ilgu Yun *

Department of Electrical and Electronic Engineering, 50 Yonsei-ro, Seodaemun-gu, Yonsei University, Seoul 120-749, Republic of Korea

ARTICLE INFO

Article history:
Received 23 August 2011
Received in revised form 10 January 2012
Accepted 1 April 2012
Available online 9 May 2012

The review of this paper was arranged by Dr. Y. Kuk

Keywords:
InGaZnO
Thin-film transistors
Subgap density of states
Channel resistance

ABSTRACT

The demand for amorphous InGaZnO (a-IGZO) thin film transistors (TFTs) has increased due to their transparent properties. In this paper, we report on the relationship between the subgap density of states (DOS), field-effect mobility (μ_{FE}), and unit channel length resistance (r_{ch}) on the electrical properties of a-IGZO TFTs. The three tested structures had the same channel width/length and gate insulator thickness with different gate insulator materials, SiN_X, SiO_X, and SiO_X/SiN_X. Compared to TFTs with low subgap DOS levels, TFTs with high subgap DOS levels have low μ_{FE} values due to the relatively large r_{ch} values.

1. Introduction

Amorphous InGaZnO (a-IGZO) thin film transistors (TFTs) were developed to meet a large market demand in the display industry due to their low temperature fabrication process and use in printable and transparent electronic applications. Furthermore, a-IGZO TFTs have good electrical performance including high mobility (>10 cm^2/V) and a large drain current on–off ratio (>10^7) [1,2]. Understanding the role of subgap density of states (DOS), such as the acceptor-like subgap DOS ($g_A(E)$), is critical for analyzing the electrical characteristics of a-IGZO TFTs. For example, Lee et al. focused on the extraction of the subgap DOS in a-IGZO TFTs [3]. Hsieh et al. studied the effect of acceptor-like subgap DOS modeling parameters based on simulation fitting [4]. The unit channel length resistances (r_{ch}) and contact resistances (R_{SD}) become significant as TFTs are scaled down. Torsi et al. investigated R_{SD} for the non-ideality of ohmic devices [5]. R_{SD} has a bigger effect on electrical characteristics as the channel length decreases [6]. Since the tested structures had a 50 μm channel length, the short channel effect was negligible and the ratio of R_{SD} to R_{ch} was very low. Thus, the electrical characteristics impacted by R_{SD} were also negligible. However, only a few studies on r_{ch} have been conducted. Studies related to both the subgap DOS and the r_{ch} have not yet been conducted [3,5].

In this paper, three types of gate insulators that include SiN_X, SiO_X, and SiO_X/SiN_X were studied by modeling in order to investigate the relationship between subgap DOS, field-effect mobility (μ_{FE}), and r_{ch}. The modeling methodology for a-IGZO TFTs using technology computer-aided design (TCAD) is presented. TCAD was used to extract subgap DOS parameters while the correlation between subgap DOS and r_{ch} was analyzed to evaluate electrical performance.

2. Experiments and modeling scheme

The TFT test structures were fabricated on a glass substrate with a 250-nm-thick Mo gate that was deposited by sputtering. Three different gate insulators were deposited on the gate metal by plasma enhanced chemical vapor deposition (PECVD). The 40-nm-thick a-IGZO channel was deposited via sputtering using a polycrystalline $In_2Ga_2ZnO_7$ target. The source and drain electrodes were then deposited by sputtering with a Mo target. The TFT channel width was 100 μm and the length was 50 μm. The information for the three test structures is summarized in Table 1. The gate insulator thickness was the same for the three test structures.

The electrical characteristics of a-IGZO TFTs were measured using Keithley 236 source measure units. The drain bias was set at 10.1 V while the gate bias was swept from −5 V to 15 V in

* Corresponding author. Tel.: +82 2 2123 4619; fax: +82 2 313 2879.
E-mail address: iyun@yonsei.ac.kr (I. Yun).

0038-1101/$ - see front matter © 2012 Elsevier Ltd. All rights reserved.
http://dx.doi.org/10.1016/j.sse.2012.04.029

Table 1
Structure information for the three test structures.

Structure name	Total thickness (Å)	Layers (thickness, Å)	$\mu_{FE(MAX)}$ ($cm^2\ V^{-1}\ s^{-1}$)
S1	2000	SiN_X(2000)	3.68
S2	2000	SiO_X(2000)	5.79
S3	2000	SiO_X(1000)/SiN_X(1000)	6.8

0.2 V steps. A commercial ATLAS device simulator modeled the average value of the initial transfer characteristics [7]. Four acceptor-like subgap DOS modeling parameters (N_{TA}, W_{TA}, N_{GA}, and W_{GA}), the constant electron mobility (MU_N), and the channel carrier concentration ($C_{carrier}$) were used to build the TFT model. The acceptor-like subgap DOS represented by the linear superposition of exponential and Gaussian functions can be modeled as [4]:

$$g_A(E) = N_{TA} \times \exp\left(\frac{E - E_c}{W_{TA}}\right) + N_{GA} \times \exp\left[-\left(\frac{E_{GA} - E}{W_{GA}}\right)^2\right], \quad (1)$$

where N_{TA} is the conduction band edge intercept density, W_{TA} is the characteristic decay energy, N_{GA} is the total DOS, E_{GA} is the Gaussian distribution peak energy, and W_{GA} is the characteristic decay energy [7]. As Hsieh et al. indicated, N_{TA} and W_{TA} have the same effect on the direction of the tail states. The effects are similar to the variation of N_{GA} and W_{GA} in the Gaussian distribution part of Eq. (1). To compare the overall parameter value changes, two parameters were selected for both the tail and the Gaussian distribution. The former is represented by W_{TA} and the latter is represented by W_{GA}. Due to the identical channel fabrication processes, $C_{carrier}$ was assumed to be the same for all test structures. Three parameters were fixed in the model. $C_{carrier}$ was $1 \times 10^{16}\ cm^{-3}\ eV^{-1}$, N_{TA} was $1 \times 10^{18}\ cm^{-3}\ eV^{-1}$, and N_{GA} was $1 \times 10^{16}\ cm^{-3}\ eV^{-1}$. MU_N was assumed to be constant for the a-IGZO channel modeling under the assumption that channel properties did not change significantly during device operation [8]. It is reasonable to assume that MU_N represents the different properties of gate insulators that only varied between the three test structures [9].

The experimentally measured μ_{FE} was calculated by:

$$\mu_{FE} = \frac{G_m}{\left(\frac{W}{L}\right) C_i V_{DS}} \quad (2)$$

where G_m is the transconductance, C_i is the gate capacitance per unit area, and V_{DS} is the drain bias. In this paper, the maximum μ_{FE} ($\mu_{FE(MAX)}$) is defined as the maximum value among the extracted μ_{FE} within the range of the measured bias. It represents the measured mobility while MU_N represents the simulated mobility. The $\mu_{FE(MAX)}$ values for S1, S2, and S3 are 3.68 $cm^2\ V^{-1}\ s^{-1}$, 5.79 $cm^2\ V^{-1}\ s^{-1}$, and 6.8 $cm^2\ V^{-1}\ s^{-1}$, respectively.

3. Results and discussion

3.1. Relationship between Subgap DOS and μ_{FE}

Fig. 1a depicts the initial measured and simulated transfer curves at V_{DS} = 10.1 V for S1, S2, and S3. Fig. 1a shows that the turn-on voltage (V_{on}) of S1 is lower than that of all the other structures. Since the modeling parameter W_{GA} has a strong impact on the turn-on voltage (V_{on}) and the transfer curve [9], it is reasonable that the W_{GA} of S1 is smaller than that of S2 and S3. The subthreshold swing (S_{SUB}) of S1 is also bigger than that of S2 and S3. Corresponding to S_{SUB}, W_{TA} can handle the on-current (I_{on}) and S_{SUB} by controlling the tail states. It is obvious that S1 has the biggest W_{TA} among the test structures. Nitrogen incorporation into silicon oxide is thought to enhance S_{SUB} for S3, resulting in the smallest W_{TA} value. The on-current (I_{on}) of S3 is slightly greater than that of S2 and S1. Wanga et al. indicated that nitrogen incorporation in oxide dielectrics causes atomic nitrogen

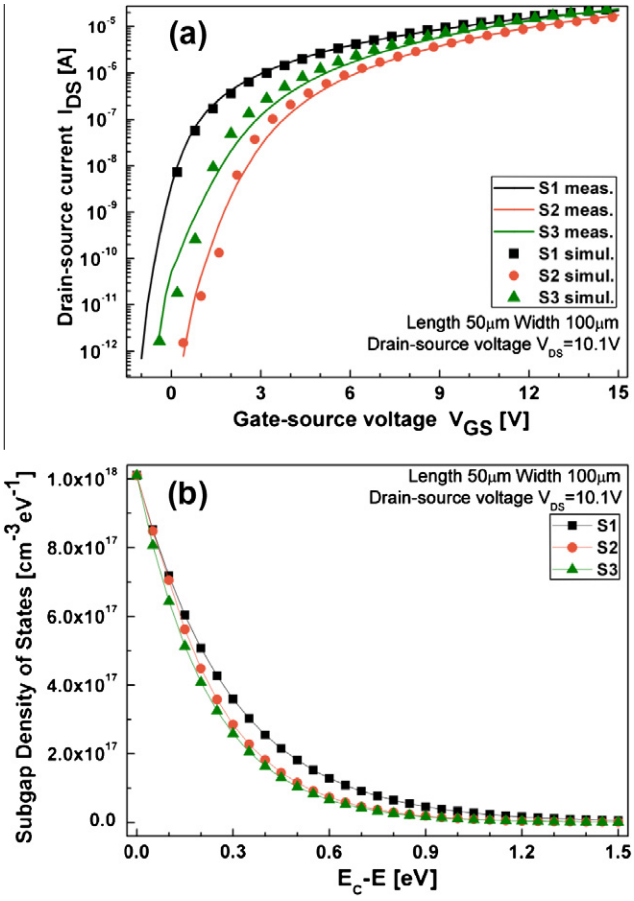

Fig. 1. Modeling results for the test structures. (a) Measured (lines) and simulated (symbols) transfer curves and (b) subgap density of states (DOS) for S1, S2, and S3.

to passivate oxygen vacancies in the oxide dielectrics, resulting in better performance [10]. The remaining modeling parameter, MU_N, is related to channel mobility. It is important to note that I_{on} of S3 is the greatest because it has the highest MU_N value, although the W_{TA} of S3 is not the smallest. The extracted values for MU_N, W_{TA}, W_{GA}, and the subgap DOS when E_c–E = 1.5 eV are summarized in Table 2.

Fig. 1b represents the calculated subgap DOS for S1, S2, and S3 by substituting the extracted values of the modeling parameters in Eq. (1). As shown in Fig. 1b, the subgap DOS is slightly larger in S2 than in S3 due to the effect of passivating oxygen deficiencies in S2, as S2 contains more oxygen deficiencies [10]. Using the subgap DOS, the relationship between simulation results and measurements can be verified.

$$\mu_{FE} = \mu_n \left(\frac{n_{free}}{n_{induced}}\right), \quad (3)$$

where μ_n represents band mobility, n_{free} represents free electron concentration, and $n_{induced}$ represents the total induced charge in the channel [11,12]. Here, μ_n is equivalent to the mobility term denoted in our simulation by 'MU_N'. The simulated μ_{FE} can be obtained by substituting the modeling data into the right-hand side of Eq. (3). n_{free} is the extracted modeling data with the optimized subgap DOS parameters (which are optimized W_{TA}, N_{TA}, W_{GA}, and N_{GA}, as listed in Table II). $n_{induced}$ is also extracted from the modeling data without considering the subgap DOS values to express the total induced charge in the channel. The ratios of n_{free} to $n_{induced}$ for S1, S2, and S3 are 0.791, 0.854, and 0.849, respectively. All considered data were obtained when V_{GS} = 15 V. Simulated μ_{FE} values for S1, S2, and S3 are 4.50, 6.55, and 7.47, respectively. Fig. 2 shows the measured